J Physiol 589.11 (2011) pp 2887–2899

The Journal of Physiology

Volume regulation in mammalian skeletal muscle: the role of sodium–potassium–chloride cotransporters during exposure to hypertonic solutions

Michael I. Lindinger[1], Matthew Leung[1], Karin E. Trajcevski[2] and Thomas J. Hawke[2]

[1]*Department of Human Health and Nutritional Sciences, University of Guelph, Guelph, ON, Canada N1G 2W1*
[2]*Department of Pathology and Molecular Medicine, McMaster University, 1200 Main St W. Hamilton, ON, Canada L8N 3Z5*

Non-technical summary During moderate to high intensity exercise, there is a net flux of solute-poor fluid into contracting skeletal muscle. This raises plasma osmolarity, and non-contracting skeletal muscle and other tissues lose water to the vascular compartment to help maintain blood volume. The loss of water from these non-contracting tissues causes the cells to shrink. For many tissues the shrinkage of the cells activates the sodium–potassium–chloride cotransporter (NKCC) which is situated in the plasma membrane. Activation of the NKCC reduces the volume loss and functions to restore cell volume in order to prevent cell damage and maintain cellular function. We show that this is also the case for mammalian skeletal myocytes and that the necessary sodium and chloride gradients to maintain NKCC activity depend on the continued activity of the sodium pump (Na^+,K^+-ATPase).

Abstract Controversy exists as to whether mammalian skeletal muscle is capable of volume regulation in response to changes in extracellular osmolarity despite evidence that muscle fibres have the required ion transport mechanisms to transport solute and water *in situ*. We addressed this issue by studying the ability of skeletal muscle to regulate volume during periods of induced hyperosmotic stress using single, mouse extensor digitorum longus (EDL) muscle fibres and intact muscle (soleus and EDL). Fibres and intact muscles were loaded with the fluorophore, calcein, and the change in muscle fluorescence and width (single fibres only) used as a metric of volume change. We hypothesized that skeletal muscle exposed to increased extracellular osmolarity would elicit initial cellular shrinkage followed by a regulatory volume increase (RVI) with the RVI dependent on the sodium–potassium–chloride cotransporter (NKCC). We found that single fibres exposed to a 35% increase in extracellular osmolarity demonstrated a rapid, initial 27–32% decrease in cell volume followed by a RVI which took 10–20 min and returned cell volume to 90–110% of pre-stimulus values. Within intact muscle, exposure to increased extracellular osmolarity of varying degrees also induced a rapid, initial shrinkage followed by a gradual RVI, with a greater rate of initial cell shrinkage and a longer time for RVI to occur with increasing extracellular tonicities. Furthermore, RVI was significantly faster in slow-twitch soleus than fast-twitch EDL. Pre-treatment of muscle with bumetanide (NKCC inhibitor) or ouabain (Na^+,K^+-ATPase inhibitor), increased the initial volume loss and impaired the RVI response to increased extracellular osmolarity indicating that the NKCC is a primary contributor to volume regulation in skeletal muscle. It is concluded that mouse skeletal muscle initially loses volume then exhibits a RVI when exposed to increases in extracellular osmolarity. The rate of RVI is dependent on the degree of change in extracellular osmolarity, is muscle specific, and is dependent on the functioning of the NKCC and Na^+, K^+-ATPase.

(Received 1 February 2011; accepted after revision 7 April 2011; first published online 11 April 2011)
Corresponding author M. I. Lindinger: Department of Human Health and Nutritional Sciences, University of Guelph, Guelph, ON, Canada N1G 2W1. Email: mlinding@uoguelph.ca

Abbreviations EDL, extensor digitorum longus; RVI, regulatory volume increase.

DOI: 10.1113/jphysiol.2011.206730

Introduction

During moderate to high intensity exercise, there is an increase in plasma osmolarity due to the net flux of solute-poor fluid into contracting skeletal muscle (Lindinger *et al.* 1994). In response to the increase in extracellular osmolarity, non-contracting skeletal muscle and other tissues lose volume to the vascular compartment which helps to defend blood volume (Lundvall, 1972). In many cells of the body (e.g. renal epithelial cells, hepatocytes), this rapid, pronounced osmotic efflux of water and resulting cellular shrinkage activates solute transport mechanisms (e.g. sodium–potassium–chloride cotransporter; NKCC) to increase the intracellular concentration of osmolytes and restore cell volume, a sequence of responses termed the regulatory volume increase or RVI (Lang *et al.* 1998; O'Neill, 1999).

Controversy exists however as to whether skeletal muscle fibres are capable of RVI. The evidence in support of skeletal muscle volume regulation is scant (Sitdikov *et al.* 1991; Sen *et al.* 1995; Lindinger *et al.* 2002; Gosmanov *et al.* 2003*b*) with most reports presenting data showing that skeletal muscle behaves as a nearly ideal osmometer (van Mil *et al.* 1997; Ferenczi *et al.* 2003; Fraser *et al.* 2005; Pickering *et al.* 2009; reviewed by Usher-Smith *et al.* 2009). While skeletal muscle may be subjected to significant volume loss for short periods of time in order to maintain plasma volume, it would seem counterproductive to be unable to undergo RVI given that chronic (hours) cellular dehydration leads to protein catabolism and apoptosis (Lang *et al.* 1998). Therefore, it should not be surprising that skeletal muscle fibres have the ability to regulate volume (Urazaev, 1998) consistent with the physical presence of the NKCC (Fu *et al.* 1999; Wong *et al.* 1999).

Therefore, it was the purpose of the present study to characterize the magnitude and time course of RVI responses of mouse soleus (slow-twitch, soleus) and extensor digitorum longus (fast-twitch, EDL) muscles and single fibres during imposed extracellular hyperosmotic stress. A secondary purpose was to investigate the functional role of the NKCC in these RVI responses. To undertake these studies, single EDL muscle fibres were loaded with the fluorescent dye, calcein, and underwent time-lapse imaging with light and fluorescence images taken throughout the osmotic challenges. A correlation between fibre width (measured with light microscopy) and fluorescence intensity was established and allowed for the study of RVI using intact muscles loaded with calcein. Our results clearly demonstrate that skeletal muscle undergoes a rapid volume loss (order of seconds) in the face of hyperosmotic stress, which is followed thereafter by a slow RVI (order of minutes) towards pre-stress volume. We further demonstrate that the RVI in skeletal muscle is dependent on functioning NKCC ion transporting proteins.

Methods

Ethical approval

The animal handling and experiments were performed in accordance with the guidelines of the Canadian Council on Animal Care and with the approval of the University of Guelph's Animal Care Committee. Adult (2–4 months old) male and female C57bl/6 mice (Charles River Laboratories, Quebec, Canada) were housed at the University of Guelph in light and temperature controlled quarters. Food and water were provided *ad libitum*. Prior to removal of muscles, each mouse was anaesthetized by acute exposure to increasing ambient CO_2 and humanely killed by cervical disarticulation when unconscious. The EDL and soleus muscles were carefully removed from the mouse and immediately placed in dissecting solution (see below) at room temperature.

Single fibre experiments

In order to validate that the increase in fluorescence intensity observed during exposure of intact muscle to increased extracellular osmolarity is correlated to decreases in cell volume we used intact, isolated single muscle fibres from mouse EDL muscles (Hawke *et al.* 2003, Shortreed *et al.* 2009). We studied fibres from four mice, and each fibre was assessed for changes in fluorescence and width at two distinct areas of the fibre, thus providing two replicates per fibre. Briefly, intact EDL muscles were placed in a sterile-filtered collagenase solution (0.2% w/v Type I collagenase, Sigma-Aldrich, Mississauga, ON, Canada) in Dulbecco's modified Eagle's medium (DMEM; Invitrogen, Burlington, ON, Canada). Following collagenase digestion, single fibres were obtained by repeated trituration of fibre bundles until many single fibres were visible. The wells of a six-well plate were treated with 10% Matrigel (BD Biosciences, Mississauga, ON, Canada) in low glucose DMEM for 1 min, rinsed with phosphate-buffered saline (PBS; Invitrogen) and refilled with 1.5 ml of low glucose plating medium. Plating medium consisted of low glucose DMEM with 10% horse serum (Sigma-Aldrich) and 0.5% chick embryo extract (MP Biomedicals) passed through a 0.2 μm nylon filter. Four to six single fibres were placed into each of two wells and the plate placed in an incubator (5% CO_2, 95% O_2) for at least 60 min at 37°C in order to allow time for fibres to adhere to the Matrigel. Calcein-AM (Invitrogen) was added to the wells containing fibres to achieve a calcein concentration of 3.2 μM and allowed to incubate for 25 min. Following incubation, the wells were gently rinsed 3 times for 1 min each to remove calcein, followed by addition of 1.5 ml fresh, calcein-free low glucose DMEM.

Plates containing fibres were taken to the microscopy suite and maintained at room temperature (20 ± 1°C) for the duration of the experiments. The plate containing fibres was placed onto the stage of a Nikon Eclipse TE2000U inverted microscope and fibre position (x–y–z coordinates) were programmed into software that allowed sequential movement between landmarks at fixed intervals. Two cycles of images were obtained using full spectrum light followed by a third cycle using fluorescence imaging (excitation at 491 nm with emission collected at 521 nm). Digital images of each landmark were collected at 6–12 s intervals for a duration of 60 min.

Three cycles of baseline images were collected, then extracellular osmolarity was raised by up to 35% by adding the appropriate volume of 1 M sucrose to the well, followed by gentle swirling. This procedure required ∼20 s and image collection was re-initiated 30 s after addition of sucrose. Images were quantified for fibre width and intensity using Adobe Photoshop software. Each fibre was imaged in two distinct microscope fields, and each of these was assessed at two locations for width and intensity. The width and intensity measures for each image were obtained as far apart as possible (120–170 μm) within a relatively straight section of the fibre within the field of view. Depending on fibre orientation, between 150 and 200 μm of fibre was present within the field of view. No measurements were obtained less than 200 μm from a fibre end.

Intact muscle experiments

Carefully removed muscles were pinned at approximately resting length, determined by micrometre measurement, to the bottom of a Sylgard (Dow-Corning, Burlington, ON, Canada) coated glass Petri dish containing dissecting solution (mM): 136.5 NaCl; 5 KCl; 0.5 $MgCl_2$; 0.4 NaH_2PO_4. Sutures (5–0 black braided surgical suture Deknatel silk) were secured to both tendon ends and each muscle was suspended on a wire clip at resting length in a 1.6 ml tube containing 1.4 ml of calcein-AM loading solution (dissecting solution with 2.84 μM calcein-AM (Invitrogen) in DMSO, such that the final DMSO concentration was 0.256%) for 45 min while rocking in the dark. Muscles were then rinsed 3 times in Tyrode solution (mM): 121 NaCl; 5 KCl; 0.5 $MgCl_2$; 0.4 NaH_2PO_4; 1.8 $CaCl_2$; 5.5 D-glucose (dextrose); 24 $NaHCO_3$; 0.3 Hepes; with a final bovine serum albumin of 22.7 μM (Shetty *et al.* 1985) and an osmolarity of 269–274 mosmol l^{-1}.

The muscle to be studied was placed into a quartz cuvette that was pump-perfused with Tyrode solution gassed with 5% CO_2, 20% O_2, 75% N_2 using a disc oxygenator to obtain a solution pH of 7.4 ± 0.05 and P_{CO_2} of 40 ± 3 mmHg. Ion and gas concentrations were confirmed using a NOVA Statprofile 9 blood gas and ion analyser (NOVA Biomedical, Waltham, MA, USA). The bottom suture of the muscle was looped under a wire hook attached to the bottom of the cuvette holder. The top suture was attached to an isometric force transducer (Harvard Apparatus; model: 60-2995) and length adjusted to obtain 1 g of tension prior to starting the experiment. A 45 min quiescent period allowed for equilibration of osmotically active ions between the intracellular and extracellular compartments, allowing that muscle volume may have been affected by the activity of stretch activated ion channels (Niu & Sachs 2003).

The muscle was excited at 491 nm with a single beam. The light emitted at 90 deg right and 90 deg left of the excitation light was collected at 521 nm. Lenses directing light at the right and left sides of the muscle were manually adjusted to maximize fluorescence emission from each side of the muscle. A different group of muscle fibres was sampled from each side of the muscle for each experiment, resulting in two replicates from most muscles. Data from each photomultiplier tube were sampled at a frequency of 10 Hz, displayed on the monitor and stored for later analysis. The natural fluorescence of the muscle without calcein, autofluorescence, was about 6–10% that of calcein-loaded muscles.

Estimate of number of fibres sampled

Penetration of light into biological tissues decreases exponentially with increasing depth of tissue. Average penetration depth of light at wavelengths of 450, 500 and 550 nm (bracketing the wavelengths (491 and 521 nm) used in the present study) has been measured in living rabbit skeletal muscle (Wilson *et al.* 1985). Penetration depth is defined as the depth at which the intensity of the light has decayed to 1/e of its surface value. Light at the wavelengths used in the present study has relatively low absorbance, and yielded an average penetration depth of 2.3 mm across these wavelengths, with an absorption coefficient of 0.012 mm^{-1} (Wilson *et al.* 1985). Light at the appropriate wavelengths was obtained from broad-band light emitted from a 1000 W Xe arc lamp (Wilson *et al.* 1985), whereas in the present study broad-band light intensity was only 75 W. Penetration is a function of intensity and thus, by direct scaling, in the present study we estimate a penetration depth of 0.17 mm, assuming negligible absorbance by the bathing medium. It is unlikely that fibres below this penetration depth contributed to the observed changes in calcein fluorescence. Using a mean fibre diameter of 35 μm for mouse skeletal muscle (Louboutin *et al.* 1993), a penetration depth of 170 μm equals a depth of 4.86 fibres.

The soleus and EDL fibres have an average cross sectional area of 1 mm^2 at the site of the light beam, which

was 2.7 mm in diameter. Therefore the entire face of the muscle facing the incident light beam was illuminated, which therefore illuminated 28.5 surface fibres of 35 μm diameter. Assuming a cylindrical geometry of the intact muscle at the region of illumination, the total number of fibres effectively penetrated by light totals 70. Of these fibres, each emission monochromator would detect light from 35 fibres. As some of the incident light will penetrate the lateral edges of the intact muscle, this could increase the total by a maximum of 10 fibres for each monochromator (side of the muscle). It is therefore estimated that each monochromator measured the responses from 40–45 muscle fibres of average 35 μm diameter.

When reporting the number of observations for the experiments described below, we report first the number of muscle sides measured (up to 2 sides per muscle), followed by the number of muscles (up to 2 muscles per mouse, followed by the number of mice). Thus, samples from both sides of a given muscle were not averaged, but taken as a separate sample that contributed to the overall *n*.

Increased extracellular osmolarity

Each muscle underwent two challenges in sequence. The first challenge consisted of a smaller increase in osmolarity than occurred in the second challenge. Paired treatments were performed with the following step increases in extracellular osmolarity: 5 and 30% or 35%, 10 and 25% or 35%, 15 and 20% (Fig. 1; $n = 6$–8 muscles from 6–8 mice). A 15 min period of recovery in normotonic solution followed the first challenge to allow for muscles to approach the original steady state volume (Frigeri *et al.* 1998; Ferenczi *et al.* 2003, B. D. Stephenson and M. I. Lindinger, unpublished observations). Data were collected during the final 5 min of this recovery period to provide baseline data for the second osmotic challenge. Step increases in osmolarity were accomplished by adding an appropriate volume of 1 M NaCl into the cuvette using a syringe pump. Cuvette contents were continuously mixed with a magnetic stir bar.

NKCC inhibition

The bumetanide (Sigma-Aldrich) solution was prepared by dissolving the powder in dimethyl sulfoxide to make a 20 mM stock solution. An appropriate volume of the stock solution was added to the cuvette to obtain a free concentration of 0.14 mM (Lindinger *et al.* 2002). In the experiments comparing control with bumetanide pretreatment experiments (SOL: $n = 20$ sides from 10 muscles from 10 mice SOL; EDL: $n = 8$ sides from 4 muscles from 4 mice), muscles were exposed to an increase in extracellular osmolarity ($\sim$125 mosmol l^{-1} using 1 M NaCl) and fluorescence was measured. Osmolarity of the bath was increased by adding 1 M NaCl into the cuvette using a syringe pump. Following completion of RVI response by the muscle, approximated by approach to a new steady state volume, data collection was terminated. The cuvette solution was removed and immediately refreshed with fresh Tyrode solution containing bumetanide and the muscles incubated in the presence of bumetanide for 30 min (Fig. 1). After the inhibitor incubation period, the cuvette solution was replaced with fresh Tyrode solution without bumetanide. The presence of bumetanide in the solution created an unusually high background fluorescence when excited at 521 nm which masked changes in muscle fluorescence, and therefore sustained NKCC inhibition was not methodologically feasible during the period of osmotic challenge.

Na^+,K^+-ATPase inhibition

The ouabain (Sigma-Aldrich) solution was prepared by dissolving the powder in Tyrode solution to make an 18 mM stock solution. An appropriate volume of the stock solution was added to the cuvette to obtain a concentration of 1.79 mM (Hawke *et al.* 1999). In the experiments comparing control with ouabain pretreatment experiments (SOL: $n = 16$ sides from 8 muscles from 8 mice SOL; EDL: $n = 12$ sides from 6 muscles from 6 mice), muscles were exposed to an increase

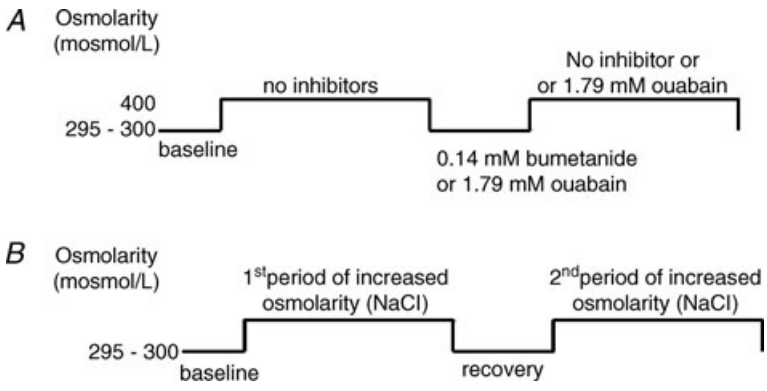

Figure 1. Design of intact muscle experiments. *A*, experimental protocol for performing experiments in the absence and presense of 1.79 mM bumetanide (NKCC inhibitor) and ouabain (Na^+,K^+-ATPase inhibitor). *B*, experimental protocol for performing the dose response to increased extracellular osmolarity.

in extracellular osmolarity (~125 mosmol l^{-1} using 1 M NaCl) and fluorescence was measured. Following completion of RVI response by the muscle, data collection was terminated, the cuvette solution was removed and immediately refreshed with fresh Tyrode solution containing ouabain, and the muscles were incubated in the presence of ouabain for 30 min (Fig. 1). After the inhibitor incubation period, the cuvette solution was replaced with fresh Tyrode solution without ouabain. In additional experiments using EDL only ($n = 8$ sides from 4 muscles from 4 mice) ouabain was retained during the second period of increased osmolarity.

Calculations

A portion of the intracellular calcein contributes to the change in fluorescence caused by changes in cellular volume (Crowe *et al.* 1995). We also found, using single fibres, that the cellular calcein fluorescence signal was inversely proportional to cell volume. Based on Crowe *et al.*'s (1995) formula, we calculated relative cell volume (V_t/V_o) as:

$$V_t/V_o = [(F_o/F_t) - F_{bkg}]/(1 - F_{bkg}) \quad (1)$$

where F_{bkg} is average background fluorescence, F_o is average fluorescence of baseline, and F_t is fluorescence at time t, with F_{bkg} calculated at 0.43 (range of 0.29 to 0.68) for the present study. Application of the calculation to single fibre fluorescence data resulted in a statistically identical fit, but the time course of the fluorescence-determined volume responses visually differed from that of the width-determined volume responses. To rectify this, we linearly correlated the 'corrected' fluorescence-determined volume response with that for width, and further 'corrected' the fluorescence data using the linear regression equation.

$$\%\ \text{change (width)} = 11.254 \pm 0.946 + (1.264 \pm 0.043 \times \%\ \text{fluorescence change}) \quad (2)$$

The resultant fit in the time course of responses using both methods was statistically and visually identical. These equations were used to calculate the volume responses of intact muscle based on fluorescence data.

Statistics

For the intact muscle experiments, the volume responses were analysed using a two-way ANOVA with respect to time and treatment, or with respect to treatment and muscle type. When a significant F ratio was obtained, a one-way ANOVA with Holm–Sidak *post hoc* test was performed to identify differences between means. For the single fibre experiments, linear regression analysis was performed to assess the relationship between fibre width and fluorescence intensity. Significance was accepted at $P \leq 0.05$. Data are reported as means ± SEM.

Results

Single fibre experiments

Optimal loading of the intracellular fluorescent volume indicator calcein-AM was achieved within 25 min of incubation. An increase of extracellular osmolarity resulted in a rapid increase in fluorescence intensity and decrease in fibre width, and this was followed by a gradual return of fluorescence and width towards baseline values (Fig. 2). The time course of width and normalized cell volume responses in fibres exposed to a step increase in extracellular sucrose are shown in Fig. 3*A*. When the fluorescence data were expressed in the same way as the width data (1 – [initial – time t/initial]) the dashed line was obtained. The discrepancy between the dashed line and width data is based, in part, on intracellular compartmentalization of calcein such that a portion of the calcein fluorescence is not sensitive to volume change (Crowe *et al.* 1995). When Crowe's equation was used to calculate normalized cell volume with our experimentally determined F_{bkg}, (0.43), the continuous line was obtained (Fig. 3*A* and *B*). Figure 3*B* shows the results of expressing the fluorescence data in two additional ways. When fluorescence data were expressed as the ratio of baseline to time t fluorescence (F_o/F_t; dashed-dotted line) the result clearly underestimated the magnitude of cellular volume decrease as determined from width. When the data were transformed using Crowe's equation and their correction (0.67) for trapped fluorescence, the dotted line resulted, which clearly overestimated the normalized volume response.

In Fig. 3*A*, the data representing the continuous line were not statistically different (one way ANOVA) from the width data, despite poorly representing the time course of volume recovery. In order to improve the ability of using fluorescence data to assess changes in volume (as determined from width changes), a linear regression analysis was performed using these two data sets (Fig. 3*C*). Applying the terms of this regression to our 'Crowe-transformed' fluorescence data gave the line shown by filled squares in Fig. 3*D*. This combined transformation was subsequently applied to fluorescence data obtained using intact muscles (below).

Intact muscle experiments

Having validated and refined the use of fluorescence intensity as a metric for volume regulation in skeletal muscle, we sought to assess volume regulation in intact muscles (soleus and EDL). Mouse soleus single fibres

are difficult to obtain and have extremely poor viability. We therefore used intact mouse soleus and EDL muscles, loaded with calcein, to study cellular responses to a range of differing extracellular osmolarities in the absence and presence of NKCC and Na^+,K^+-ATPase inhibitors. Utilizing intact muscle served to (1) confirm the single fibre results particularly in light of the fact that the isolation of single fibres involved enzymatic digestion, which may have affected activity and functionality of cell surface transporters; and (2) allow assessment of muscles composed of differing fibre types with respect to their sensitivity to increased extracellular osmolarity and ability to regulate volume.

Very similar to the responses seen in single muscle fibres, intact muscle showed a rapid increase, followed by a gradual reduction, in cellular fluorescence when extracellular osmolarity was greater than 10 mosmol l^{-1}. Normalized cell volume was calculated from changes in fluorescence. The 35% increase in extracellular osmolarity was chosen to provide a maximal, physiologically relevant (Lindinger *et al.* 1992), stimulus for the RVI response. There were no differences between soleus and EDL in the rate and magnitude of the initial shrinkage in response to a 35% increase in extracellular osmolarity to 400 mosmol l^{-1} (Fig. 4*A*). Peak volume loss occurred in less than 10 min (400–600 s) and ranged between 20 and 30% of cell volume. The subsequent recovery of muscle volume took significantly longer in EDL than soleus and remained incomplete 20 min after initiation of the hypertonic challenge; 30–40 min was required to achieve a new steady state volume.

It was hypothesized that the RVI was affected by increased activity of the NKCC, the activity of which is maintained, in part, by the activity of the Na^+,K^+-ATPase which serves to keep intracellular [Na^+] low. In the experiment shown in Fig. 4*B*, an EDL was incubated for 30 min in the presence of 0.14 mM bumetanide to inhibit the NKCC. The extracellular solution was rapidly replaced with one having a 35% increased extracellular osmolarity, but with no bumetanide present (continuous line, Fig. 4*B*). In both EDL and soleus (not shown), pre-treatment with the NKCC inhibitor increased the magnitude of volume loss, prolonged the duration of volume loss and slowed the recovery of volume (dashed line, Fig. 4*B*).

Muscles were also incubated for 30 min with 1.79 mM ouabain to inhibit Na^+,K^+-ATPase activity. Because the Na^+,K^+-ATPase maintains the trans-sarcolemmal driving forces for inward flux of Na^+ and Cl^- by the NKCC, ouabain-induced inhibition of Na^+,K^+-ATPase activity serves as a validation for the bumetanide-induced inhibition of the NKCC trials (Lindinger *et al.* 2001). Similar to NKCC inhibition, pre-incubation with ouabain, but with no ouabain present during the period of increased osmolarity (soleus: $n = 16$ sides from 8 muscles from 8 mice soleus; EDL: $n = 12$ sides from 6 muscles from 6 mice), prolonged the duration of volume loss and slowed the recovery of volume (Fig. 4*C*). In contrast to bumetanide, pre-incubation with ouabain did not significantly affect the magnitude of volume loss. The continued presence of ouabain during the period of increased osmolarity (EDL only) largely abolished the RVI.

Dose responses to increased extracellular osmolarity

The dose–response relationship of soleus and EDL to increased extracellular osmolarity in the range of 5 to 35% was studied with respect to the magnitude of volume loss, the time required to achieve peak volume loss, the

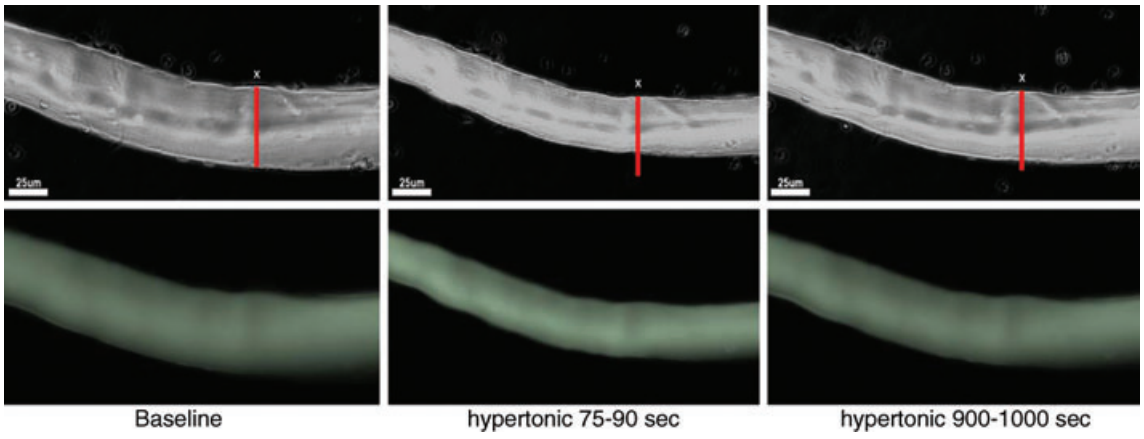

Figure 2. Myocytes lose volume when exposed to increased extracellular osmolarity and then regain volume.
Baseline; 75–90 s; 900–1000 s. Time course of fibre width (top images) and fluorescence (bottom images) in response to increased extracellular osmolarity. Cell volume loss was characterized by decrease in width simultaneous to increase in calcein fluorescence intensity (see Fig. 3).

magnitude of volume recovery and the time required to achieve peak volume recovery.

A 5% increase in osmolarity had no effect on soleus and a small effect on EDL volumes. In both muscles, the magnitude of cellular volume loss increased in proportion to increasing extracellular osmolarity (Fig. 5) as described by the equations:

$$\text{Soleus: volume loss} = -0.0135 \pm 0.0550 - (0.00720 \pm 0.00229 \times \%\ \text{osmolarity});$$
$$r^2 = 0.712;\ P = 0.035$$

$$\text{EDL: volume loss} = -0.0114 \pm 0.0243 - (0.00645 \pm 0.00109 \times \%\ \text{osmolarity});$$
$$r^2 = 0.876;\ P = 0.002$$

The EDL lost significantly more volume than soleus with up to 30% increases in extracellular osmolarity; however, the volume losses in response to the 35% increase in osmolarity were similar in the two muscles. The subsequent volume recovery was also significantly related to the increasing extracellular osmolarity in soleus, but not EDL (Fig. 5), as described by the equation:

$$\text{Soleus: volume recovery} = -0.0239 \pm 0.0328 + (0.00384 \pm 0.00136 \times \%\ \text{osmolarity});$$
$$r^2 = 0.664;\ P = 0.048$$

Also, soleus tended ($P = 0.079$) to recover 5–10% more volume than was initially lost (Fig. 5, left panel, grey bars above 0). The times to achieve peak volume loss and peak

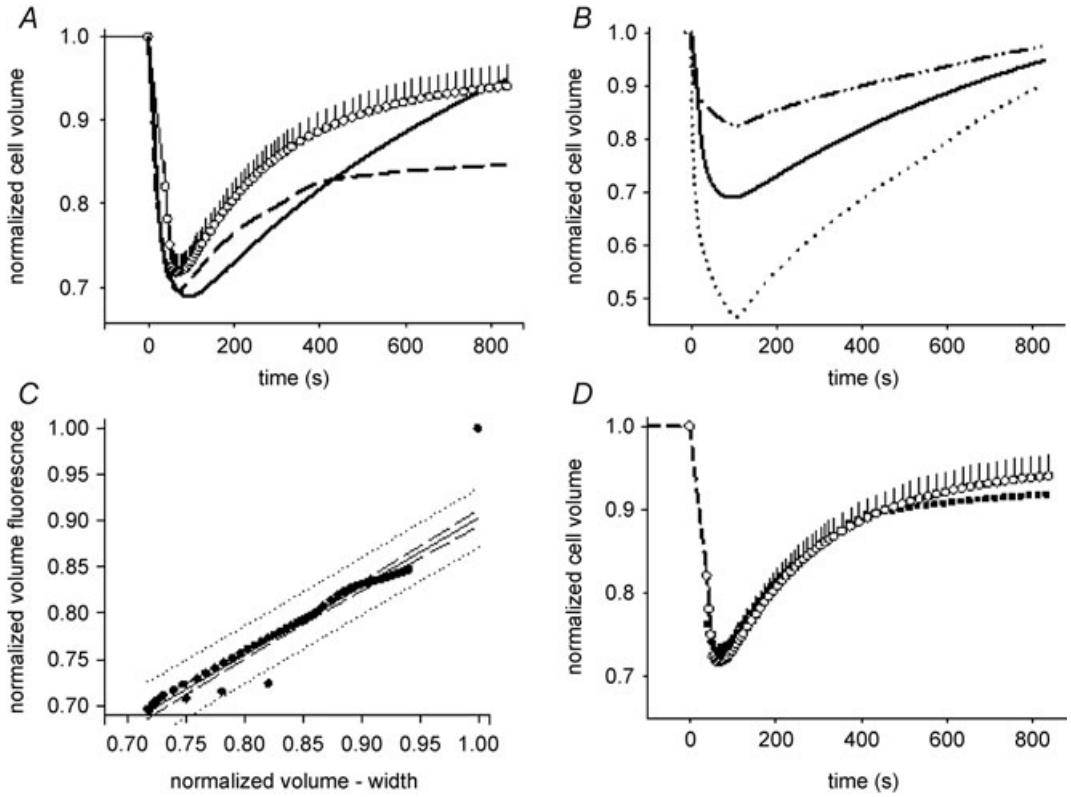

Figure 3. Equating changes in muscle calcein fluorescence with changes in cellular volume.
A, time course of change in cell volume during exposure to a 35% increase in extracellular osmolarity. Normalized cell volume was calculated using change in width (○, with SEM bars; $n = 8$ sections from 4 fibres from 2 mice; $[1 - (W_o - W_t)]/W_o$), or using change in fibre fluorescence intensity ($[1 - (F_o - F_t)]/F_o$), dashed line), and using Crowe *et al.*'s (1995) equation with our experimentally determined F_{bkg} of 0.43 (continuous line; same continuous line as in *B*). This correction for background or 'trapped' intracellular fluorescence produced a result that was not statistically different from the fibre width data, but clearly has shortcomings with respect to accurately portraying the time course of volume recovery. *B*, average ($n = 8$ sections from 4 fibres from 2 mice) change in normalized cell volume calculated as the ratio of the baseline fluorescence (F_o) : fluorescence at time t (F_t) (dashed–dotted line) and using eqn (1) using Crowe *et al.*'s (1995) F_{bkg} of 0.67 (dotted line) and our experimentally determined F_{bkg} of 0.43 (continuous line; same continuous line as in panel *A*). *C*, linear regression analysis results of fitting the 'corrected' fibre fluorescence (continuous lines of *A* and *B*) to the change in volume based on fibre width. *D*, the time course of change in cell volume calculated from change in fibre width (same data as in *A*) and from the final fluorescence data (■) corrected for F_{bkg} (0.43) and fitted using the linear regression equation.

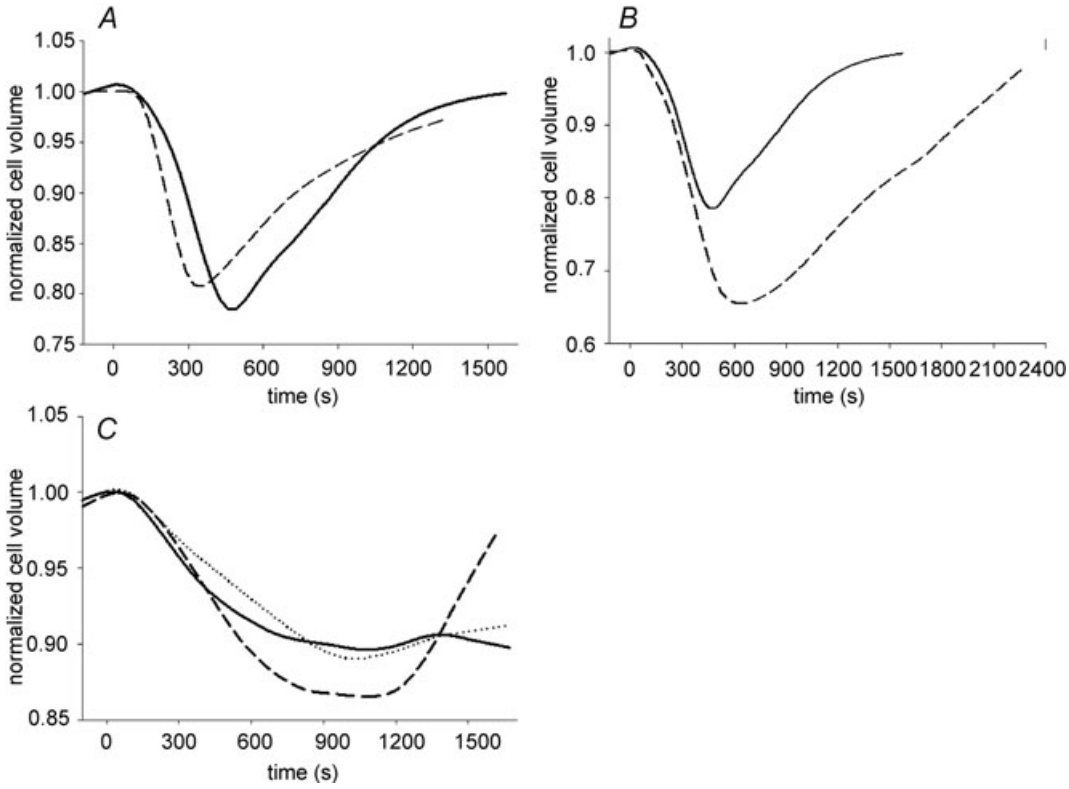

Figure 4. Fibre type differences in volume loss and RVI responses.
A, time course of normalized cell volume change in typical intact EDL (continuous line) and soleus (dashed line) muscles exposed to a 35% increase in extracellular osmolarity at 0 s. *B*, time course of normalized cell volume change in a typical intact EDL muscle (continuous line, same as in *A*) and after incubation with 0.14 mM bumetanide for 30 min prior to a 35% increase in extracellular osmolarity at 0 s in the subsequent absence (dashed line) of bumetanide. *C*, normalized volume responses from both sides of an EDL muscle (continuous and dotted lines) incubated with 1.79 mM ouabain for 30 min, followed by a step increase in extracellular osmolarity of 20 mosmol l^{-1} by addition of NaCl in the presence of ouabain at 0 s. When ouabain was not present during the period of increased osmolarity, resulting in gradual loss of inhibition of Na^+,K^+-ATPase activity, there was a delayed, though rapid, regulatory volume increase (dashed line).

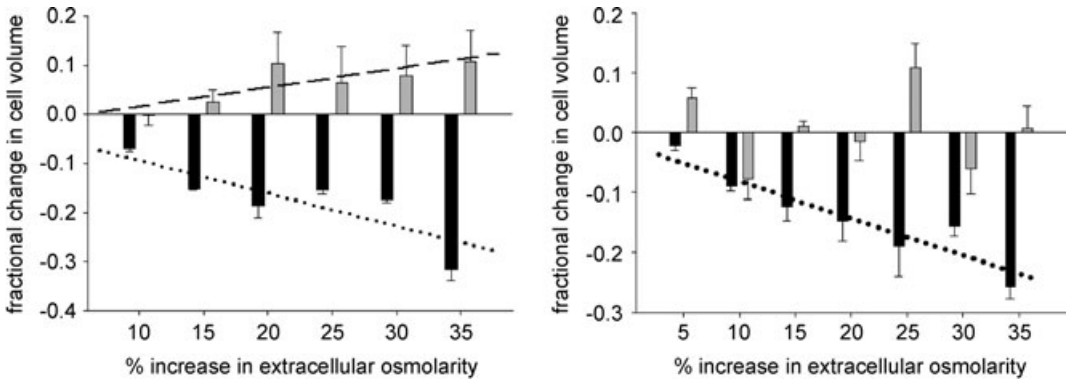

Figure 5. Peak volume loss (black bars) and volume recovery (grey bars), relative to initial baseline volume in soleus (left panel) and EDL (right panel)
The bars represent means and SEM. Values greater than 0 represent an overshoot of the volume recovery. $n = 4$ for each osmolarity, except soleus 30% where $n = 7$ and EDL 5% where $n = 3$. The lines indicate significant linear relationships between the increase in extracellular osmolarity and peak volume loss and recovery for SOL, and only for volume loss for EDL. See text for additional details.

volume recovery were variable and not different between treatment doses.

Discussion

Utilizing two unique methodologies (isolated single fibres and intact muscles), we demonstrate here that that muscles made to shrink by exposure to a hyperosmotic environment actively regained their volume by a process dependent on increased NKCC activity and Na^+,K^+-ATPase activity. The present results also indicate that cell volume is more tightly regulated in slow twitch postural muscle fibres than in fast twitch locomotory fibres. This observation is consistent with the ability of fast fibres to tolerate large changes in both extracellular and intracellular environments, including intracellular ion and metabolite concentrations during high intensity exercise (Lindinger & Heigenhauser, 1991). Finally, we demonstrated that the RVI mechanisms activated immediately upon exposure to the hyperosmotic stress as the cellular volume loss in each muscle was much less than would be expected if muscle behaved as a perfect osmometer (Usher-Smith *et al.* 2009). Taken together, our findings suggest that while non-contracting skeletal muscle will lose volume in an effort to maintain blood volume in situations that result in rapid and pronounced increases in blood osmolarity (e.g. intense exercise), volume loss from these muscles will eventually be rectified by RVI even when extracellular osmolarity remains elevated. These physiological responses may help explain the decreasing performance observed in athletes experiencing dehydration during prolonged or repeated periods of intense exercise.

Calcein as a volume indicator and muscle viability

At the cellular level, the present study used a non-invasive technique based on measurement of changes in the concentration of the intracellular fluorescent dye calcein. In addition to its use as an indicator of cellular volume, calcein is widely used as an indicator of cell viability (Tanioka *et al*. 2007). Thus, the use of calcein not only allowed us to measure RVI, but also provided us with an index of cell viability for single fibres and intact muscles as fibre death would result in a rapid decrease in fluorescence. Other indicators of fibre viability and functionality over the course of these experiments are the fact that muscles were capable of eliciting two sequential RVI responses with a recovery period between the two exposures to increased extracellular osmolarity. Excessive metabolic rundown of the muscles would result in an impaired or absent second RVI response, and this was encountered in less than 10% of experiments. We also measured ATP and phosphocreatine content in muscles put through the various experiments approximately 2.5, 5, 7.5 and 10 h ($n = 4$ soleus and 4 EDL at each time) following harvesting. There was a linear decrease over time, with ATP decreased by 22% in soleus and 35% in EDL while PCr was decreased by 77% and 71% respectively, at 10 h compared to freshly harvested muscle. We are therefore confident that the fluorescence responses in these experiments are the result of volume loss and recovery mechanisms and not the result of membrane leakage or instability.

We demonstrated that the fluorescence of calcein was inversely proportional to cell water volume changes, such that an increase in fluorescence was indicative of fibre water loss. While the time course of volume loss and increase when using calcein were statistically similar to measures of volume change using fibre width, mathematical adjustments were necessary, particularly to account for background fluorescence not sensitive to volume changes (Crowe *et al*. 1995), to overlay the two profiles perfectly. Based on these data, muscle cells appear to 'trap', on average, 43% of intracellular calcein compared to 67% by neuronal cells (Crowe *et al.* 1995). It is concluded that changes in calcein fluorescence can be used to assess volume changes in skeletal muscle fibres, as has been shown previously in other cell types (e.g. Crowe *et al.* 1995).

When comparing the kinetics of the cellular shrinkage and, in particular, the RVI responses between single fibres and intact muscle under control (no inhibitors) conditions, there was an approximate doubling of the time required for intact muscle compared to single fibres. We believe that this difference is primarily due to diffusion limitations in the intact muscle preparation, related to the fact that the emitted light was likely to have been sampled to a depth of four fibres. There will be a temporal delay in achieving increased extracellular osmolarity as fibre depth increases. Also, while the superficial most fibre layer will respond fastest, there are a greater total number of fibres in the second through the fourth cell layers from which emitted light is also detected. *In vivo*, one would expect the response of muscle cells to be more closely represented by the single fibre response, but also with an increased rate of recovery due to higher muscle temperatures *in vivo.*

Regulation of cell volume during periods of increased extracellular osmolarity

In the intact muscle experiments, increased NaCl, as opposed to sucrose in the single fibre experiments, was used to increase extracellular osmolarity because increased NaCl better represents (physiologically) the increase in osmolarity that occurs with high intensity exercise. These two compounds exert slightly different effects on the magnitude of the initial volume and subsequent RVI when examined within the same muscle type (intact muscle – B. D. Stephenson & M. I. Lindinger, unpublished

observations; single fibres – M. Leung, J. Moynes & M. I. Lindinger, unpublished observations) because sucrose is completely membrane impermeant, while Cl^- rapidly equilibrates across the sarcolemma due to the high membrane conductance of Cl^-.

A hypertonic blood plasma and extracellular fluid is produced physiologically during periods of high intensity exercise (Lindinger *et al.* 1992) when arterial osmolarity increases due to the accumulation of metabolic, osmotically active molecules within contracting muscle, which swells (Lindinger & Heigenhauser, 1991; Lindinger *et al.* 1994). There are two, nearly simultaneous, fluid shifts that occur during moderate to high intensity exercise. The first is an osmotic fluid shift from the vascular compartment into contracting muscle that results in a rapid decrease in plasma volume that can exceed 600 ml (Lundvall, 1972; Lindinger *et al.* 1994). There occur consequent increases in plasma osmolarity and oncotic pressure. The second fluid shift is the net movement of fluid from non-contracting skeletal muscle and other tissues to the vascular compartment in response to increased extracellular osmotic and oncotic pressures. This second fluid shift, in essence, protects plasma and circulating blood volume, but results in volume loss within these tissues (Lundvall, 1972), similar to those described in the present study. It is evident from our findings and those of others (Lang *et al.* 1998; Urazaev, 1998) that the initial volume loss and subsequent volume gain resulting from net movement of solute into muscle cells must be linked to a mechanism that allows for the rapid osmotic flow of water out of and into cells. It is suggested that these water fluxes occur by facilitated diffusion of water across the rather impermeant sarcolemma through water channels. The membrane water channel protein aquaporin 4 (Aqp4) has been demonstrated in fast twitch mammalian skeletal muscle but may not be present in slow twitch muscle (Frigeri *et al.* 1998; Nicchia *et al.* 2007). In accordance with Antolic *et al.* (2007) and Cermak *et al.* (2009), the current observations also suggest that the EDL may be influenced to a greater extent by fluid shifts caused by altered extracellular osmolarity than soleus. When cellular volume losses occur slowly, as with prolonged sweating without fluid replacement during endurance activities, it remains unknown if and/or how muscle cells attempt to regulate volume.

Evidence supporting functions of the NKCC and Na^+,K^+-ATPase in RVI

In many, but not all, mammalian cell types the mechanism of RVI is an increased simultaneous transport of Na^+, K^+ and Cl^- into cells by the NKCC (Lang *et al.* 1998) that is secondarily sensitive to inward Na^+ and Cl^- driving forces maintained by Na^+,K^+-ATPase activity (O'Neill, 1999; Lindinger *et al.* 2002). Bumetanide, which inhibits the NKCC, impaired the initial activation of the RVI responses in both soleus and EDL upon exposure to increased extracellular osmolarity. Incubation of muscles within bumetanide prior to increased extracellular osmolarity had two effects: (1) an increased magnitude of volume loss and (2) a delayed, though complete, RVI response. The effect of bumetanide strongly implicates the NKCC in the ability of mammalian skeletal muscle cells to elicit the RVI. Furthermore, when muscles were incubated with ouabain prior to, and during, exposure to increased extracellular osmolarity, the impaired cell volume regulatory responses were markedly similar to those seen with bumetanide, though when ouabain was present during the period of increased osmolarity the RVI was effectively abolished. These results demonstrate that the activity of the Na^+,K^+-ATPase is required to sustain inward driving forces for Na^+ and Cl^- in order to maintain activity of the NKCC.

The fact that muscles incubated in the presence of bumetanide to inhibit NKCC activity did partially recover volume, albeit more slowly than controls, suggests incomplete inhibition of all functioning NKCC protein and/or the presence of other mechanisms for increasing cellular volume. At the bumetanide concentration used, the free [bumetanide] exceeded the IC_{50} for muscle NKCC activity by 10-fold (Walker *et al.* 1989; Lindinger *et al.* 2001) and therefore it is estimated that at best 95% of NKCC incorporated into the sarcolemma was inhibited. The continued osmotic stress, coupled with maintenance of trans-sarcolemmal Na^+ and Cl^- gradients sustained by the Na^+,K^+-ATPase (O'Neill, 1999) would have resulted in an increasing activity of unblocked NKCC proteins that is likely to account for the slow RVI observed. At present there are no other RVI mechanisms known in skeletal muscles, although inward amino acid transport has been implicated in other cell types (O'Neill, 1999).

Muscle-specific differences

Though EDL lost significantly more volume than soleus, there was no difference in the rate of volume loss. On the surface, this result is consistent with the presence of Aqp4 in EDL, but not soleus fibres (Frigeri *et al.* 1998; Nicchia *et al.* 2007), which would facilitate an enhanced flux of water in the fast twitch fibres. Although EDL did not recover significantly more volume than soleus, when extracellular NaCl concentration was raised, EDL took longer to recover that volume, indicating a slower rate of NKCC activity than in soleus. Furthermore, soleus showed no response to the 5% increase in extracellular osmolarity while EDL did, and the recovery volume overshoot increased linearly with increasing extracellular osmolarity in soleus, but not in EDL. This is consistent with the lower expression of NKCC in fast twitch (plantaris) compared to slow twitch (soleus) muscles of rats (Wong *et al.*

1999). Taken together these results suggest that the volume response of postural slow twitch muscle is more tightly regulated than that of the locomotory fast twitch EDL that tolerates larger volume perturbations.

The rate of volume loss was not different between soleus and EDL in any of the dose–response experiments, suggesting that the rate of volume loss is dependent on the magnitude of the tonic challenge and is not a function of muscle type or NKCC distribution. In EDL, similar to amphibian muscle (Ferenczi *et al*. 2003), volume loss increased linearly with an increase in extracellular osmolarity.

The rates and magnitude of volume recovery in response to the hypertonic challenge appears to be dependent on the degree of activation of the NKCC which, in turn, is a function of magnitude of the hypertonic challenge. The greater the hypertonic challenge to the muscle, the more rapid appears to have been the activation of the NKCC and recovery of volume, particularly in soleus where volume often recovered to above the initial volume. The end point of volume recovery, or point at which a steady state is once again achieved, must be a function of the de-activation of the NKCC. Thus, it is suggested that the recovery volume overshoot seen in soleus, but not EDL, indicates not only a greater activation of the NKCC in soleus, but also a slowed de-activation.

Mammalian skeletal muscle cells do not behave as a perfect osmometer

Antolic *et al*. (2007) showed that mammalian muscle cells lose water when exposed to a 36% increase in extracellular osmolarity. Somewhat in agreement with the present study, the equilibrium volume at 60 min after the imposed increase in extracellular osmolarity was much less than expected if muscles behaved as perfect osmometers. In addition to the present results, others (Sitdikov *et al.* 1989; Naumenko *et al*. 1999; Urazaev, 1998) have demonstrated that mammalian skeletal muscle cells do not behave as (near) perfect osmometers. Rather, and in agreement with many other mammalian cell types (Lang *et al*. 1998), the present study supports the theory that mammalian skeletal muscle cells actively increase intracellular osmolarity to match that of their extracellular environment, thereby effectively restoring at least a portion of the lost volume and cell shape. Maintenance of cellular volume and shape appears to be linked to contractile performance (Bressler, 1977; Bressler & Matsuba, 1991), and it is likely that a host of other normal functions in skeletal muscle are also volume sensitive, including metabolic activity (Cermak *et al.* 2009). It is therefore concluded that mammalian skeletal muscles actively attempt to maintain a structural set-point rather than behaving as osmometers (Lang *et al*. 1998). The roles of extracellular protein linkages and cytoskeletal elements in the activation of volume regulatory mechanisms (Pedersen *et al*. 2001) requires further investigation.

The present results differ from those obtained in single amphibian (Fraser *et al.* 2005) and mouse (van Mil *et al.* 1997; Pickering *et al.* 2009) skeletal muscle fibres which did behave as (near) perfect osmometers under their study conditions. We speculated that this apparent inability to regulate volume was associated with the absence of key serum constituents within the bathing solution (Shetty *et al*. 1985). However, when we prepared and incubated single fibres in Tyrode solution, as detailed by Pickering *et al.* (2009) and other studies, a RVI was still observed after the initial period of volume loss upon increased extracellular osmolarity (M. Leung & M. I. Lindinger, unpublished observation). What is clear is that the viability of our preparations was maintained as demonstrated both by the functioning of appropriate sarcolemmal transporters and the continued presence of our cell viability fluorophore, calcein.

Perspectives

We have previously addressed some of the physiological rationale for why skeletal muscle cells should actively regulate volume (Gosmanov *et al.* 2003*a*) and these aspects will not be reiterated here. Nonetheless, a number of recent studies have pointed to additional roles implicating skeletal muscle volume in the control of muscle metabolism (Cermak *et al.* 2009), whole body glucose homeostasis (Lang *et al.* 2009; Hallows *et al*. 2011) and blood pressure regulation (Kahle *et al.* 2010; Orlov *et al.* 2010*a*). In isolated mammalian hepatocytes, cell volume loss is associated with an increased metabolism and catabolism, whereas increased volume is associated with an anabolic effect (reviewed by Lang *et al.* 1998; Lang *et al.* 2006). In mammalian skeletal muscle cellular shrinkage is associated with increased metabolic activity (Cermak *et al.* 2009) perhaps associated with ATP requirements for restoring ion concentrations and volume.

There is increasing evidence that impaired NKCC activation is involved in the severe hyperglycaemia that can accompany diabetes mellitus. Hyperglycaemia associated with increases in circulating insulin may result in insulin-stimulated NKCC and Na^+,K^+-ATPase activities that imposes osmotic, cell volume and energetic stresses on skeletal muscle that may impact the regulation of extracellular fluid volume of the body. Insulin increases skeletal muscle NKCC activity under conditions of osmotic stress (Gosmanov & Thomason 2002). It is hypothesized that under conditions of insulin insufficiency or insulin resistance that integrated cellular functions of skeletal muscle glucose disposal, ion transport, volume regulation and energy production are dysregulated (Lang *et al*. 2009; Hallows *et al.* 2011). Finally, because skeletal

muscle NKCC activity ultimately will influence regulation of whole body extracellular fluid volume, inherited diseases affecting the regulation of the NKCC not only impair the ability of the predominant tissue of the body (skeletal muscle) to regulate its volume and ion transport processes, but is also associated with impaired fluid, ion and blood pressure regulation (Kahle *et al.* 2010; Orlov *et al*. 2010*b*).

Conclusions

Mammalian skeletal muscles are capable of RVI in response to the initial cellular shrinkage induced by exposure to physiological increases in extracellular osmolarity. In most situations of increased osmolarity, cells recovered all of the volume lost. The magnitude of the initial volume loss was also much less than if the cells behaved as perfect osmometers, indicating rapid sensing of volume loss and activation of RVI mechanisms. The RVI is bumetanide sensitive, consistent with primary involvement of the NKCC, and ouabain sensitive, consistent with a requirement of the Na^+,K^+-ATPase to maintain electrochemical driving forces for inward flux of Na^+ and Cl^-. Fast twitch (EDL) muscle lost more volume and took longer to recover volume compared to slow twitch (soleus) muscle. This suggests that volume change is more tightly regulated in slow twitch postural muscles, while fast-twitch, locomotive muscles can tolerate larger volume perturbations. Volume changes in single muscle fibres assessed from changes in calcein fluorescence and fibre width were comparable, indicating that calcein can be used in intact muscle to assess volume responses.

References

Antolic A, Harrison R, Farlinger C, Cermak NM, Peters SJ, LeBlanc P & Roy BD (2007). The effect of ectracellular osmolarity on cell volume and resting metabolism in mammalian skeletal muscle. *Am J Physiol Regul Integr Comp Physiol* **292**, R1994–R2000.

Bressler BH (1977). Isometric tension and instantaneous stiffness in amphibian skeletal muscle exposed to solutions of increased osmolarity. *Can J Physiol Pharmacol* **55**, 1208–1210.

Bressler BH & Matsuba K (1991). Tension and instantaneous stiffness of single muscle fibres immersed in Ringer solution of decreased osmolarity. *Biophys J* **59**, 1002–1006.

Cermak NM, LeBlanc PJ, Peters SJ, Vandenboom R & Roy BD (2009). Effect of extracellular osmolality on metabolism in contracting mammalian skeletal muscle in vitro. *Appl Physiol Nutr Metab* 34, 1055–1064.

Crowe WE, Altamirano J, Huerto L & Alvarez-Leefmans FJ (1995). Volume changes in single N1E-115 neuroblastoma cells measured with a fluorescent probe. *Neuroscience* **69**, 283–296.

Ferenczi EA, Fraser JA, Chawla S, Skepper JN, Schwiening CJ & Huang CLH (2003). Membrane potential stabilization in amphibian skeletal muscle fibres in hypertonic solutions. *J Physiol* **555**, 423–438.

Fraser JA, Middlebrook CE, Usher-Smith JA, Schwiening CJ & Huang CL (2005). The effect of intracellular acidification on the relationship between cell volume and membrane potential in amphibian skeletal muscle. *J Physiol* 563, 745–764.

Frigeri A, Nicchia GP, Verbavatz JM, Valenti G & Svelto M (1998). Expression of aquaporin-4 in fast-twitch fibres of mammalian skeletal muscle. *J Clin Invest* **102**, 695–703.

Fu L, Wong JA, Schneider EG & Thomason DB (1999). Unique 5′-end of a Na^+-K^+-$2Cl^-$ cotransporter-like mRNA expressed in rat skeletal muscle. *DNA Seq* **10**, 127–132.

Gosmanov AR, Lindinger MI & Thomason DB (2003*a*). Riding the tides: K^+ concentration and volume regulation by muscle Na^+-K^+-$2Cl^-$ cotransport activity. *News Physiol Sci* **18**, 196–200.

Gosmanov AR, Schneider EG & Thomason DB (2003*b*). NKCC activity restores muscle water during hypertonic challenge independent of insulin, ERK, and p38 MAPK. *Am J Physiol Regul Integr Comp Physiol* **284**, 655–665.

Gosmanov AR & Thomason DB (2002). Insulin and isoproterenol differentially regulate mitogen-activated protein kinase-dependent Na^+-K^+-$2Cl^-$ cotransporter activity in skeletal muscle. *Diabetes* **51**, 615–623.

Hallows KR, Mount PF, Pastor-Soler NM & Power DA (2011). Role of the energy sensor AMP-activated protein kinase in renal physiology and disease. *Am J Physiol Renal Physiol* (in press).

Hawke TJ, Willmets RG & Lindinger MI (1999). K^+ transport in resting rat hind-limb skeletal muscle in response to paraxanthine, a caffeine metabolite. *Can J Physiol Pharmacol* **77**, 835–843.

Hawke TJ, Jiang N & Garry DJ (2003). Absence of p21CIP rescues myogenic progenitor cell proliferative and regenerative capacity in Foxk1 null mice. *J Biol Chem* **278**, 4015–4020.

Kahle KT, Rinehart J & Lifton RP (2010). Phosphoregulation of the Na-K-2Cl and K-Cl cotransporters by the WNK kinases. *Biochim Biophys Acta* **1802**, 1150–1158.

Lang F, Busch GL, Ritter M, Volkl H, Waldegger S, Gulbins E & Haussinger D (1998). Functional significance of cell volume regulatory mechanisms. *Physiol Rev* **78**, 247–306.

Lang F, Görlach A & Vallon V (2009). Targeting SGK1 in diabetes. *Expert Opin Ther Targets* **13**, 1303–1311.

Lang F, Shumilina E, Ritter M, Gulbins E, Vereninov A & Huber S (2006). Ion channels and cell volume in regulation of cell proliferation and apoptotic cell death. *Contrib Nephrol* **152**, 142–160.

Lindinger MI, Hawke TJ, Vickery L, Bradford L & Lipskie SL (2001). An integrative, in situ approach to examining K^+ flux in resting skeletal muscle. *Can J Physiol Pharmacol* **79**, 996–1006.

Lindinger MI, Hawke TJ, Lipskie SL, Schaefer HD & Vickery L (2002). K^+ transport and volume regulatory response by NKCC in resting rat hindlimb skeletal muscle. *Cell Physiol Biochem* **12**, 279–292.

Lindinger MI & Heigenhauser GJF (1991). The roles of ion fluxes in skeletal muscle fatigue. *Can J Physiol Pharmacol* **69**, 246–253.

Lindinger MI, Heigenhauser GJF, McKelvie RS & Jones NL (1992). Blood ion regulation during repeated maximal exercise and recovery in humans. *Am J Physiol Regul Integr Comp Physiol* **262**, R126–R136.

Lindinger MI, Spriet LL, Hultman E, Putman T, McKelvie RS, Lands LC, Jones NL & Heigenhauser GJ (1994). Plasma volume and ion regulation during exercise after low- and high-carbohydrate diets. *Am J Physiol Regul Integr Comp Physiol* **266**, R1896–R1906.

Louboutin JP, Fichter-Gagnepain V, Thaon E & Fardeau M (1993). Morphometric analysis of *mdx* diaphragm muscle fibres: comparison with hindlimb muscles. *Neuromusc Disord* **3**, 463–469.

Lundvall J (1972). Tissue hyperosmolality as a mediator of vasodilatation and transcapillary fluid flux in exercising skeletal muscle. *Acta Physiol Scand* Suppl **379**, 1–142.

Naumenko NV, Uzinskaya KV, Shakirzyanova AV, Urazaev AKh & Zefirov AL (1999). [Adenosine triphosphoric acid as a factor of nervous regulation of $Na^+/K^+/2Cl^-$ cotransport in rat skeletal muscle fibres]. *Bull Exp Biol Med* **147**, 583–586.

Nicchia GP, Mola MG, Pisoni M, Frigeri A & Svelto M (2007). Different pattern of aquaporin-4 expression in extensor digitorum longus and soleus during early development. *Muscle Nerve* 35, 625–631.

Niu W & Sachs F (2003). Dynamic properties of stretch-activated K^+ channels in adult rat atrial myocytes. *Prog Biophys Mol Biol* **82**, 121–135.

O'Neill WC (1999). Physiological significance of volume-regulatory transporters. *Am J Physiol Cell Physiol* 276, C995–C1011.

Orlov SN, Gossard F, Pausova Z, Akimova OA, Tremblay J, Grim CE, Kotchen JM, Kotchen TA, Gaudet D, Cowley AW & Hamet P (2010*a*). Decreased NKCC1 activity in erythrocytes from African Americans with hypertension and dyslipidemia. *Am J Hypertens* **23**, 321–326.

Orlov SN, Tremblay J & Hamet P (2010*b*). NKCC1 and hypertension: a novel therapeutic target involved in the regulation of vascular tone and renal function. *Curr Opin Nephrol Hypertens* **19**, 163–168.

Pedersen SF, Hoffmann EK & Mills JW (2001). The cytoskeleton and cell volume regulation. *Comp Biochem Physiol A Mol Integr Physiol* **130**, 385–399.

Pickering JD, White E, Duke AM & Steele DS (2009). DHPR activation underlies SR Ca^{2+} release induced by osmotic stress in isolated rat skeletal muscle fibres. *J Gen Physiol* **133**, 511–524.

Sen CK, Hanninen O & Orlov SN (1995). Unidirectional sodium and potassium flux in myogenic L6 cells: mechanisms and volume-dependent regulation. *J Appl Physiol* **78**, 272–281.

Shetty RPM, Krishna DJ & Macchia DD (1985). Effects of albumin on resting membrane potential of toad semitendinosus muscles. *Pflügers Arch* **404**, 83–85.

Shortreed KE, Krause MP, Huang JH, Dhanani D, Moradi J, Ceddia RB & Hawke TJ (2009). Muscle-specific adaptations, impaired oxidative capacity and maintenance of contractile function characterize diet-induced obese mouse skeletal muscle. *PLoS ONE* **10**, e7293.

Sitdikov RF, Urazaev AKh, Volkov EM, Poletaev GI & Khamitov KhS (1989). [Effects of hyperosmolarity and furosemide on resting membrane potentials and skeletal muscle fibre volume in rats] (in Russian). *Biull Exsp Biol Med* **108**, 563–566.

Sitdikov RF, Urazaev AKh, Volkov EM, Poletaev GI & Khamitov KhS (1991). [Neurotrophic control of the ionic regulation mechanisms for intracellular water content in muscle fibres of mammals]. *Neirofiziologiia* **23**, 625–628.

Tanioka H, Hieda O, Kawasaki S, Nakai Y & Kinoshita S (2007). Assessment of epithelial integrity and cell viability in epithelial flaps prepared with the epi-LASIK procedure. *J Cataract Refract Surg* **33**, 1195–1200.

Urazaev AKh (1998). [The sodium-potassium-chloride cotransport of the cell membrane]. *Usp Fiziol Nauk* **29**, 12–38.

Usher-Smith JA, Huang CL & Fraser JA (2009). Control of cell volume in skeletal muscle. *Biol Rev Camb Philos Soc* 84, 143–159.

van Mil HGJ, Geukes Foppen RJ & Seigenbeek Van Heukelom J (1997). The influence of bumetanide on the membrane potential of mouse skeletal muscle cells in isotonic and hypertonic media. *Br J Pharmacol* **120**, 39–44.

Walker PC, Berry NS & Edwards DJ (1989). Protein binding characteristics of bumetanide. *Dev Pharmacol Ther* **12**, 13–18.

Wilson BC, Jeeves WP & Lowe DM (1985). *In vivo* and *post mortem* measurements of the attenuation spectra of light in mammalian tissues. *Photochem Photobiol* **42**, 153–162.

Wong JA, Fu L, Schneider EG & Thomason DB (1999). Molecular and functional evidence for Na^+-K^+-$2Cl^-$ cotransporter expression in rat skeletal muscle. *Am J Physiol Regul Integr Comp Physiol* **277**, 154–161.

Author contributions

The intact muscle experiments were performed in MIL's lab, University of Guelph. The single fibre experiments were performed in TJH's former lab at York University, Toronto, Canada. MIL designed all experiments, assisted in all experiments, data collection and analysis and was primarily responsible for writing the paper. TJH was involved in the design, execution and analysis of the single fibre experiments and contributed to writing the paper. ML was involved in performing the single fibre experiments, data collection, image analysis and data analysis. KET harvested muscles and obtained viable single fibres, taught the technique to ML, and contributed to writing the manuscript. All authors approved the final version of the manuscript.

Acknowledgements

We thank Ben Stephenson and Kate Henderson for their assistance with the intact muscle experiments, Jasmin Moradi for the provision of excellent single fibres and Dan Atkinson for excellent assistance with the single fibre microscopy. This study was funded by grants from to M.I.L. and T.J.H. from Natural Sciences and Engineering Research Council of Canada (NSERC).